Chapter 3
A Multi-agent Model of *Physarum*

> "...but a drop or bubble may realise in an instant the whole apparatus of curves.... bearing witness to the fact that one common law is obeyed by every point or particle of the system. Where the underlying equations are unknown to us, as happens in so many natural configurations, we may still rest assured that kindred mathematical laws are being automatically followed, and rigorously obeyed, and sometime half-revealed."

(D'arcy Wentworth Thompson, 1917)

3.1 Introduction

This chapter describes the multi-agent model of *Physarum*, which is a particle based reaction-diffusion pattern mechanism behaving as a collective virtual material. The base model behaviour is described and its pattern formation properties explored in an evaluation of model parameters.

3.2 Motivations for Model Choice

We wish to approximate the biological patterning behaviour and computational behaviour of the *Physarum* plasmodium. Furthermore we wish to reproduce certain features of the plasmodium: simple components, distributed behaviour (and computation), oscillatory phenomena, and morphological adaptation. In this section we describe the motivation for a fine-grained, spatially implemented, material-based approach.

3.2.1 Granularity

When deciding on a modelling strategy we must choose a level of detail, or granularity, at which to simulate the desired process. We must choose a level

J. Jones, *From Pattern Formation to Material Computation,*
Emergence, Complexity and Computation 15, DOI: 10.1007/978-3-319-16823-4_3

which captures the desired behaviour, does not make too many experimental assumptions, yet which does not model irrelevant details. Whilst we seek simplicity we must bear in mind the words of caution (attributed to Einstein), that models should be: "...as simple as possible (but no simpler)". For spatially implemented models the granularity choice is particularly important since it impacts directly on factors such as the lattice representation and the base behaviour encoded in the model. For example, for a biological organism, we might consider the following possible grain levels for *Physarum*: *atomic-molecular-chemical-actomyosin-plasmalemma-plasmodium.*

We wish to implement the self-organisation phenomena which result in the distributed, de-centralised and emergent behaviour of the plasmodium. Choosing a high-level approach would force us to make too many modelling assumptions about the causal factors generating these phenomena. We must therefore choose a granularity which is fine enough to show emergent properties, which is extensible and is computationally tractable. A similar difficulty occurs at the simpler fine-grained levels; the genetic and biochemical interactions which occur in *Physarum*, although well studied, are not yet completely understood, nor computationally tractable. Although lower levels of grain appear conceptually simpler to implement (since the individual behavioural steps are smaller and simpler), it is not possible to directly specify the higher level observed phenomena, such as the foraging and adaptation behaviour of *Physarum*, in terms of lower granularity since a complex behaviour pattern such as "migrate towards stimulus" is beyond the scope of such a simple instruction set.

3.2.2 A Continuum of Material Patterning

By exploiting 'material properties' we mean the behaviour that a material *collectively* demonstrates under certain environmental conditions, as opposed to the behaviour of its individual constituent parts. Many materials exhibit complex patterning in response to environmental stresses, including fracture patterns in ceramics [153], drying materials [154], and dielectric breakdown [155]. However this patterning is typically non-mutable. To model adaptive patterning in *Physarum* the chosen mechanism must be capable of adjusting its pattern over time, i.e. the patterning must be more flexible. We can consider patterning as a continuum where, at one extreme, there is rigid 'one shot' patterning to relieve stresses in the material. Moving further along the continuum we observe greater flexibility or adaptability in the patterning, as observed in leaf venation where Couder et al. argue that part of the mechanism must exhibit visco-elastic properties to form and maintain patterning [29]. Even more flexibility results in patterning as seen in gels [156], lipid networks [111] and soaps and froths [157, 158]. At the extreme end of this scale there are materials which maintain cohesion but little patterning, such as oils and water. We can use this continuum of material patterning as an

inspiration to devise a mechanism which allows mobility, complex patterning, adaptability, shows cohesion, and is stable over time.

3.2.3 Material-Like Properties in Collectives

In some instances, loose aggregates of materials or individuals can also demonstrate material-like patterning, for example in agitated granular media [145], crowd behaviour in emergencies [159], liquid-like flows in ant colonies [160], or flocking patterns of birds ([106]). In such examples the physical forces responsible for cohesion in real materials are replaced by indirect coupling of individuals provided by direct contact, visual information, or chemotactic cues. This suggests that by incorporating such a coupling method we can gain material-like properties within loose collectives.

3.2.4 Spatial Implementation

As prototype non-classical computing devices utilise physical properties of their substrates, the choice of a spatial representation for the *Physarum* model using a non-classical approach is logical. However, this also requires that the mechanisms used in the model must also be incorporated spatially, as opposed to abstracted numerically. For our approach we utilise a 2D lattice based model to represent the structure of the plasmodium and an isomorphic diffusive lattice to represent the flux within the plasmodium as described below.

3.3 A Multi-agent Virtual Material Approach

The model used to approximate the behaviour of *Physarum* is based on the multi-agent approach. A population of very simple particle-like mobile software agents interact within a 2D diffusive lattice comprising their environment. The approach used is in the tradition of fine-grained and 'bottom-up' models, where macroscopic phenomena emerge from the interactions between simpler components at the microscopic scale.

The level of granularity chosen corresponds to the movement interactions within the plasmodium gel/sol matrix. By choosing this level we are removing the complexity of sub-atomic, atomic and molecular details. It is important to note that we are also removing the 'layer' of chemical interactions within the plasmodium. It is these interactions which generate the motive force for the protoplasmic streaming within the plasmodium. We remove this layer partially because it is not yet fully understood biologically or energetically, and partially because it has already been demonstrated that this layer may be approximated by conceptualising the plasmodium as a membrane bound sub-excitable reaction diffusion system [4]. Therefore we assume that the

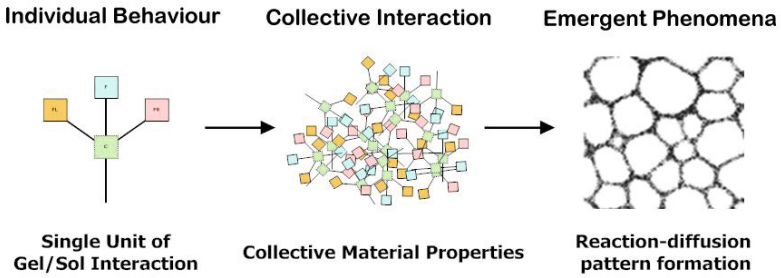

Fig. 3.1 Multi-agent based approach approximates gel / sol plasmodium interactions. left) single agent particle, middle) collective mass of agents, right) complex pattern formation.

chemical transformations, over the surface of, and within the plasmodium provide a contractile force acting upon individual hypothetical units of gel/sol comprising the actomyosin network of the plasmodium. It is the coupling and flux within the gel/sol matrix which we explicitly model in this report and which, we will show, is sufficient to explain the complex behaviour of the *Physarum* plasmodium. The approach is summarised in Fig. 3.1.

3.3.1 Model Overview

The model specifically addresses the generation of network formation and adaptation, oscillatory phenomena and transport phenomena exhibited by *Physarum* . We divide the model into three parts, beginning with the base 'material' behaviour of network formation and adaptation. The material properties of the model must be emergent, distributed within the material and utilise a mechanism of self-organised dynamical pattern formation. The base behaviour of the model is then expanded to reproduce growth and adaptation of the *Physarum* plasmodium. This allows the exploration of how foraging and adaptation is influenced by nutrients within the environment. The third part of the model is the addition of oscillatory behaviour. As with the base model behaviour, oscillatory phenomena in the model must be an emergent property and thus arise from the interactions within the material. The addition of subsequent behaviours to the base model behaviour must not impinge upon previous behaviours, which are subsumed within the new additions. Results pertaining to each are included in separate chapters for clarity.

Firstly we must reproduce the basic material properties of the plasmodium, i.e. a virtual material which is capable of complex dynamical pattern formation and adaptation from the particle collective. The material properties must be distributed within the collective and emerge from the interactions between the simple components, requiring no special component parts. In this chapter we summarise the behaviour and parametric evaluation of the

base material and its response to simple analogues of environmental stimuli by the formation of transport networks between the stimuli.

3.3.2 The Building-Block of a Virtual Plasmodium

The model framework is a particle representation of reaction-diffusion (RD) processes. Unlike classical RD models, which are composed of the interactions of at least two simulated activator/inhibitor reactants in a diffusive environment, there is only a single representative reactant: a mobile particle which senses and deposits simulated chemoattractant as it moves within a diffusive environment. The combined sensing and deposition of chemoattractant represent an active mode of RD computation — the particle both senses and modifies the diffusion field. This is an alternative to a passive mode where the computation is achieved purely by wavefront propagation and in which the particles only follow the diffusion field [73]. In general terms the framework belongs to the LALI (Local Activation and Long range Inhibition) approaches which encompasses RD methods [141], and specifically agent based approaches into LALI patterning [144].

The virtual plasmodium is comprised of a population of agent particles, whose population size is given by p (or, as a percentage of lattice area, $\%p$). The diffusive lattice is represented by a discrete two-dimensional floating point array. Agent particle positions are stored on a coupled discrete lattice (isomorphic to the diffusive lattice) but, in an attempt to overcome the limitations of movement of the discrete representation, the particles also store an internal floating point positional and angular representation which is rounded to a discrete value to compute movement updates and sensory inputs. A single particle, and an aggregation of particles, is related to the *Physarum* plasmodium in the following way: The plasmodium syncytium is conceptualised as an aggregate of identical components. Each particle represents a hypothetical unit of gel/sol interaction. Gel refers to the relatively stiff sponge-like matrix composed of actin-myosin fibres and sol refers to the protoplasmic solution which flows within the matrix.

The structure of the protoplasmic network is indicated by the collective pattern of particle *positions* and the flow of sol is represented by the collective *movement* of the particles. The resistance of the gel matrix to protoplasmic flux of sol is generated by particle-particle movement collisions. As an analogy one can imagine a tightly crowded population within a room, the confined space generating collisions and thus resistance to movement. Local amplification of flux is provided by particle – particle sensory coupling. An analogical description of the coupling can be understood if the population in the room were coupled by linking hands with close neighbours, thus when one neighbour moves it creates a local increase in flow (and a temporary vacant space) which attracts nearby particles.

3.3.3 Agent Particle Sensory Behaviour

A single agent represents a hypothetical particle of *Physarum* plasmodium gel/sol structure. When a particle moves, the movement can be said to represent the protoplasmic flux of sol. When a particle is not able to move it can be said to represent the immobile gel matrix. The general morphology of an agent and its basic underlying algorithm is illustrated in Fig. 3.2. Each agent is typically initialised at a randomly chosen unoccupied and habitable location and with a random orientation (from zero to 360°, freeing the agent from the restrictive rectangular architecture of the underlying lattice). The agent receives chemotactic sensory stimuli from its environment (chemoattractant levels stored in the diffusive lattice) via three forward sensors (Fig. 3.2a) and the agent responds to differences in the local environment chemoattractant levels by altering its orientation angle to face the locally strongest concentration by rotating left or right about its current position (Fig. 3.2b). The sensor offset distance (in pixels) is represented by the *SO* parameter and it can be considered as a scaling parameter. The agent is forward biased, i.e. only the sensors directly in front of the agent's current position are used to influence its behaviour, thus ensuring a continuous movement-based dynamic.

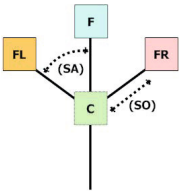

(a)

```
[Sensory stage]

- Sample chemoattractant map values
- if (F > FL) && (F > FR)
        - Continue facing same direction
- Else if (F < FL) && (F < FR)
        Rotate by RA towards larger of FL and FR
- Else if (FL < FR)
        Rotate right by RA
- Else if (FR < FL)
        Rotate left by RA
- Else
        Continue facing same direction
```

(b)

Fig. 3.2 Base agent particle morphology and sensory stage algorithm. (a) Illustration of single agent, showing location 'C', offset sensors 'FL','F','FR', Sensor Angle '*SA*' and Sensor Offset '*SO*', (b) simplified sensory algorithm.

3.3.4 Agent Particle Motor Behaviour

The motor behaviour of the particles represents the flux of material within the plasmodium. The motor behaviour operates in either non-oscillatory or oscillatory modes (Fig. 3.3). The non-oscillatory mode represents an idealised movement with no build up of forces within the plasmodium due to obstruction. As will be demonstrated, this mode generates smooth evolution of network structure with no obstruction and hence no emergence of oscillatory phenomena. This mode is used to assess the network evolution under ideal conditions and is described below.

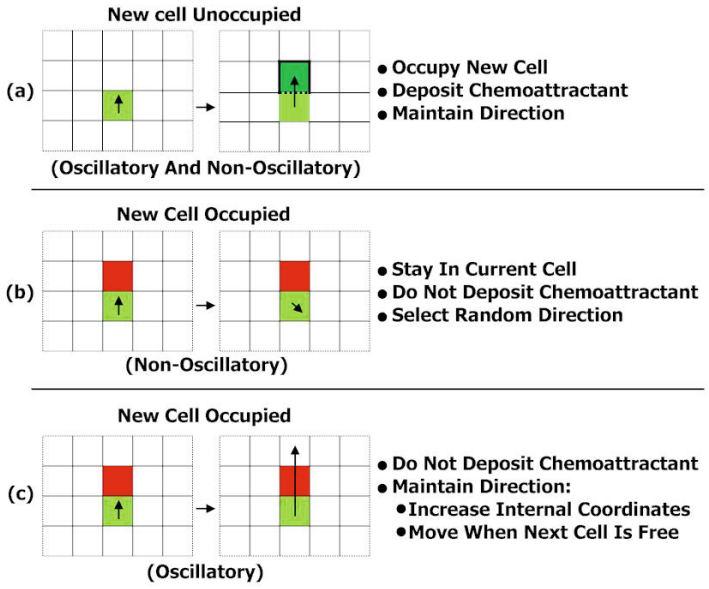

Fig. 3.3 Agent particle motor behaviour under non-oscillatory and oscillatory conditions. (Top) movement to vacant site, (Middle) behaviour if site is occupied (non-oscillatory), (Bottom) behaviour if site is occupied (oscillatory).

At each execution step of the scheduler every agent attempts to move forward in the lattice by the value SS (default value of 1) in the current direction. After every agent has attempted its move, the entire population executes its sensory behaviour. If the movement is successful (i.e. if the next site is not occupied) the agent moves to the new site and deposits a constant chemoattractant value into the diffusive lattice, given by the value Dep_t, with a default value of 5 units (Fig. 3.3a). In the default, non-oscillatory condition, if the movement is not successful the agent remains in its current position, no chemoattractant is deposited, and a new orientation is randomly selected (Fig. 3.3b). The selection of a new direction if the agent is blocked prevents deadlock in the lattice and clustering of agents.

In the oscillatory motor condition, however, we wish to approximate the build up of resistance within the plasmodium. If a chosen site is occupied the agent remains in the current cell and increments an internal coordinate counter facing the same direction. When a site becomes free the agent occupies the new site, moving past the blocked site (Fig. 3.3c). This simple mechanism results in temporary blockages until the particles are able to 'push past' each other and results in the emergence of surging movement which is described in more detail in chapter 15.

3.4 Growth and Adaptation of the Virtual Plasmodium

Growth and adaptation of the particle model population is implemented using a simple method based upon local measures of space availability (growth) and overcrowding (adaptation by population reduction). This is undoubtedly a gross simplification of the complex factors involved in growth and adaptation of the real organism (such as metabolic influences, nutrient concentration, waste concentration, slime capsule coverage, bacterial contamination etc.). However the simplification renders the population growth and adaptation more computationally tractable and the specific parameters governing growth and shrinkage are at least loosely based upon real environmental constraints. Growth and shrinkage states are iterated separately for each particle and the results for each particle are indicated by tagging Boolean values to the particles. Any particles tagged for growth/shrinkage are considered by the framework scheduler at regular intervals of periods given by G_f and S_f, the growth/shrinkage frequency (default value, every 3 scheduler steps). The growth and shrinkage rules for each particle are given below, with default values indicated in brackets:

Let n be the number of particles within local window radius G_w (9) centred around the current particle position (x, y). Let *rand* be the random number generated between 0 and 1 with uniform distribution. $Gmin$ (0) and $Gmax$ (10) are the local crowding size, outside which growth cannot occur. $pDiv$ (1) is a probability that a particle will multiply if the conditions are suitable.

if $(n > Gmin$ AND $n \leq Gmax)$ AND $(rand < pDiv)$
divideparticle = True
Else
divideparticle = False

At each scheduler division step any particles tagged with the *divideparticle* flag attempt to multiply by executing the following pseudocode:

If (*divideparticle*)
Choose random cell in window radius 1 around current particle position, if available.
Create new particle in this cell.

The shrinkage rules for each particle are given as:

Let n be the number of particles within local window radius S_w (5) centred around current particle position (x, y). Let $Smin$ (0) and $Smax$ (24) be the local crowding size outside which the particle will be removed.

if ($n > Smin$ AND $n \leq Smax$)
shrinkparticle = False
Else
shrinkparticle = True

At each scheduled shrinkage step, any particles tagged with 'shrink' are removed.

3.5 Representing the Agent Population Environment Habitat

The environment is implemented spatially using a discrete 2D lattice. Each addressable site (x, y) on the lattice refers to a unique location which may store a single agent particle. Each (x, y) address may also address values in isomorphic lattices representing flux within the plasmodium and the locations of nutrients, hazards and toxins. The flux of sol within the plasmodium is represented by a floating point value in a diffusive lattice and referred to as generic 'chemoattractant'.

3.5.1 Habitat Configuration

To represent the experimental environment the lattice is configured by supplying the scheduler with a 2D greyscale image. The image represents a configuration map for the experiment. A coding system is used to denote particular environmental features with particular greyscale levels, including habitable background regions, experimental borders, inhabitable regions, hazardous regions, nutrient stimuli locations, and specific inoculation sites. An initial population of agent particles, representing a small fragment of plasmodium, is created (size p, where p is the initial number of particles) and initialised with random orientations at either background regions or specific inoculation sites.

3.5.2 Representation of Nutrient Chemoattractants

Simulated chemoattractant nutrient source stimuli whose position and concentration are stored in the configuration map are projected to the diffusive lattice at every step of the scheduler. The concentration of the chemoattractant stimuli (in arbitrary units) is given by the greyscale intensity at the lattice site. The concentration can be adjusted by multiplication with a global weighting parameter $Proj_d$.

3.5.3 Representation of Nutrient Chemorepellents

Physarum is known to migrate away from certain compounds [161, 82]. To reproduce the effect of chemorepellent stimuli at specific sites, negatively weighted values, Rep_d, are used to project features in the environment at these locations. Because the agent particle behaviour is to orient towards stronger concentration regions, particles will move away from the chemorepellent regions. Under growth and adaptation conditions, an agent particle is not able to divide if it is within a repellent region.

3.5.4 Representation of Response to Illumination

Physarum plasmodium tends to avoid areas under illumination [162]. This phenomenon has been used to affect the structure of the plasmodium transport network and the directional migration of plasmodia [163, 84]. To implement this phenomenon in the model we include a specific hazard value in the lattice. Illuminated areas in the environment are tagged with the hazard value. If an agent is located within an illuminated region, denoted by a window L_w centred about the agent (default value 5), the value of sensed chemoattractant in the sensor is reduced by multiplying it by a weighting factor L_d, whose value may be between zero and 1. Lower values of L_d reduce the value of sensed chemoattractant in the illuminated region and the collective is thus less attracted to the illuminated region. Under growth and adaptation conditions, an agent particle is not able to divide if it is within an illuminated region.

3.5.5 Diffusion Mechanism

The chemoattractant stimuli are diffused by means of a simple mean filter kernel of size D_w, (typically 3×3). The diffusion operator is applied to all cells simultaneously via pseudo-parallelism methods. The diffusing chemoattractant values may be damped by the value D_d (typically 0.1) to adjust the concentration of the diffusion gradient away from the nutrient source. (mean of D_w, multiplied by $(1 - D_d)$, smaller values of D_d resulting in less damping of diffusion). The persistence of the diffusion gradient corresponds to the quality of the nutrient substrate of the plasmodium's environment (for example the different growth patterns seen in damp filter paper and nutrient-rich agar substrates). Differences in the stimulus concentration (greyscale value in the configuration map) and stimulus area (the size of nutrient source), affect both the steepness, and propagation distance of the diffusion gradient and affect the growth patterns of the synthetic plasmodium.

If the movement of agent particles represents the flux within the tube network, the frequency of diffusion, given by the parameter D_f, represents the persistence of the tube network itself. Typically the value is 1, i.e. diffusion

is carried out after every scheduler step, and results in faster adaptation of the tube network. A larger value of D_f will result in less frequent diffusion and greater persistence of the tube network.

3.5.6 Gradient Suppression and Nutrient Consumption

Suppression of the production of nutrient gradients when nutrients are engulfed by the model plasmodium is achieved by a simple method. At each iteration of the scheduler the local neighbourhood E_w (default value 5), centred around every position in the lattice, is checked to see if it is occupied by a particle and, if so, the projection of nutrient to the diffusive map is reduced by multiplying by a damping factor E_d, between 0 and 1.

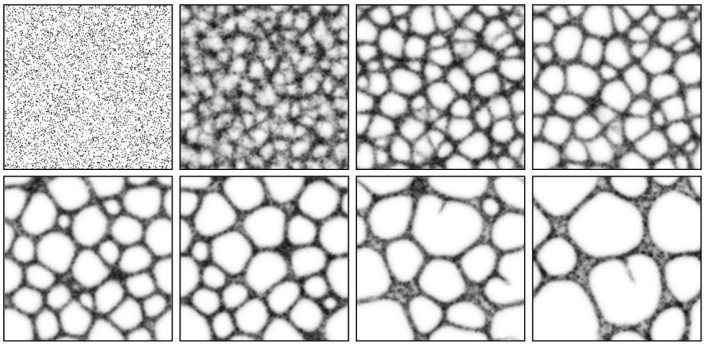

Fig. 3.4 Spontaneous formation and evolution of transport networks. Lattice 200×200, $\%p15$, SA 22.5°, RA 45°, SO 9, Images taken at: 2, 22, 99, 175, 367, 512, 1740 and 4151 scheduler steps.

Consumption of nutrients is achieved in a similar way: At each iteration of the scheduler the local neighbourhood C_w (default value 5), centred around every position in the lattice, is checked to see if it is occupied by a particle. If any consumable nutrients are within this area the nutrient level is decremented by a value C_d (larger values of C_d result in faster consumption). Decrementing the nutrient level reduces the concentration of chemoattractant projected onto the diffusive lattice. When the nutrient level at a particular part of the lattice reaches zero no further projection occurs at this point. For experiments on simulated nutrient-rich substrates which simulate an agar substrate rich in nutrients (for example cornmeal agar), it is also possible to specify higher concentrations of nutrients (relating to oat flake positions) which are not consumed as quickly as the background substrate.

3.6 Self-Assembly of Emergent Transport Networks

We begin the examination of the behaviour of the particle population by studying fixed population sizes and the initiation of network formation. This allows us to explore and evaluate the base behaviour of the model and explore its parameters. After initialisation at random locations and orientations, the randomly distributed agent population spontaneously forms network trails (see Fig. 3.4, and supplementary video recordings for this chapter).

The spatial patterns are formed by, and composed of, the bi-directional flow of agents (see supplementary recording of 'naked' particles with visible sensors). The network forms because agents are attracted to the strongest local source of chemoattractant. Individual agents secrete chemoattractant when they move forwards successfully. The chemoattractant diffuses into the lattice, ensuring that nearby agents are attracted to the area and a positive feedback (Local Activation) loop is formed. Lateral inhibition is not explicitly encoded and is generated by the local depletion of the substrate: Particles within low concentration regions are attracted to nearby regions of high concentration and the number of agents in the low concentration regions further diminishes, thus further reducing attraction of such regions to the particles. Because the agent particles only deposit chemoattractant after successful movement, and because the agents have a forward biased sensory apparatus, static clustering of agents is avoided and a dynamic network is formed.

3.6.1 Network Motifs

The dynamical nature of the network exhibits complex emergent properties. Smaller cyclic areas of the network gradually contract and disappear. As the smaller cyclic areas disappear, larger lacunae predominate and grow as the smaller regions shrink. Occasionally, however, a bifurcation will appear in one of the network edges and a new path 'sprout' will branch out across the dividing space of a single lacuna. When the gap is breached there is a surge of movement as the two moving flows are connected. This surge includes an outflow from the far edge to the moving sprout as agents within the trail at the far edge are attracted to the chemoattractant flow of the sprout.

The result is a dynamical network whose shape is constantly changing but whose composite parts remain the same in number. For the default sensor parameters (SA 22.5°, RA 45°) the network never stabilises completely (although temporarily stable regimes have been observed, see supplementary recordings). The complexity of the network evolution is also affected by changes in network structure. For example, the collapse of a cyclic structure by contraction, redistributes agents into different parts of the network. This affects network flow in local areas, further changing the configuration. A simple relationship is thus formed: The change in network structure (e.g. branching, closing) affects local agent flux which, in turn, affects the network structure ... and so on. The dynamical evolution of the network with the

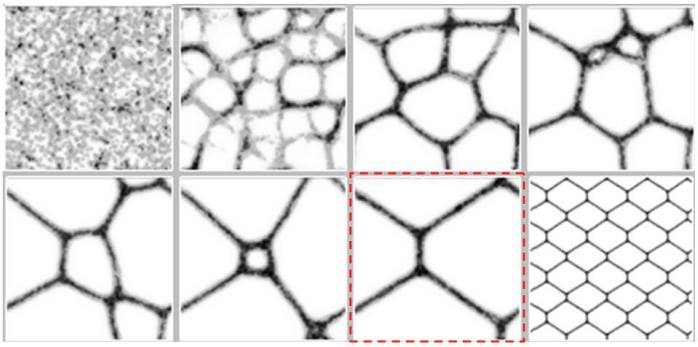

Fig. 3.5 Stable minimising network approximates hexagonal tiling. Final image shows approximate hexagonal tiling of stable state image 7 (dashed).

default parameters is because the rotation angle is significantly greater than the sensor angle. The wide rotation angle places the sensors away from the main gradient stream after a rotation. If this is coupled with random changes in direction (due to agent-agent collisions) a new bifurcation can become stabilised and reinforced by agent flow.

When both SA and RA are 45° the same initial complex network evolution is observed but the bifurcation and sprouting of new trails does not persist. In this case the lacunae gradually become larger as the smaller cycles are closed. Eventually a simple network is formed which, when tiled, approximates a regular hexagonal tiling (Fig. 3.5).

The networks evolve without any pre-patterning of the environment and different configurations appear at each run. The shape of the network is influenced by the random initial distribution of agents and the random initial orientation of the agents. The chemoattractant trails that emerge when the agents move quickly break symmetry when, for example, one area by chance accrues more chemoattractant than another. Once agents aggregate in trails, unoccupied areas become more devoid of chemoattractant (as the trails diffuse away), further amplifying the disparity (and attraction for) the areas. Like classical approaches to reaction-diffusion pattern formation, there is a reaction component (the deposition of chemoattractant by agents and the orientation towards stronger concentration). There is also a diffusion component (the diffusion of the chemoattractant from the deposition sites). However, unlike classical morphogen based models of Turing-type pattern formation, there is no explicit inhibition mechanism present. Note that without the presence of a diffusion mechanism, the patterning would be dependent to a large extent on the initial distribution and orientation of the agents.

3.6.2 Bi-directional Transport — Shuttle Streaming

The mass behaviour of the agent population shows collective network formation. When observing a single agent's movement, however, the movement does not follow the smooth flow that might be expected. The movement is hesitant and moves backwards and forwards as it progresses along a particular path. To investigate the characteristics of single agent movement the movement of a single particle was recorded. The network was a single path with periodic boundary conditions and the particle position was recorded over the course of 4000 scheduler steps and the result is shown in Fig. 3.6. The movement trend to the right side is punctuated by direction changes, indicative of shuttle-streaming. Example of such movement can be seen in the supplementary recordings. Due to the lack of resistance in particle flow under the non-oscillatory motor behaviour condition of the model, to-and-fro oscillations in particle flow tend not to accumulate. Under oscillatory conditions, however, interruption in particle flow can aggregate, resulting in stronger shuttle-streaming phenomena (see chapter 16, section 16.2.2).

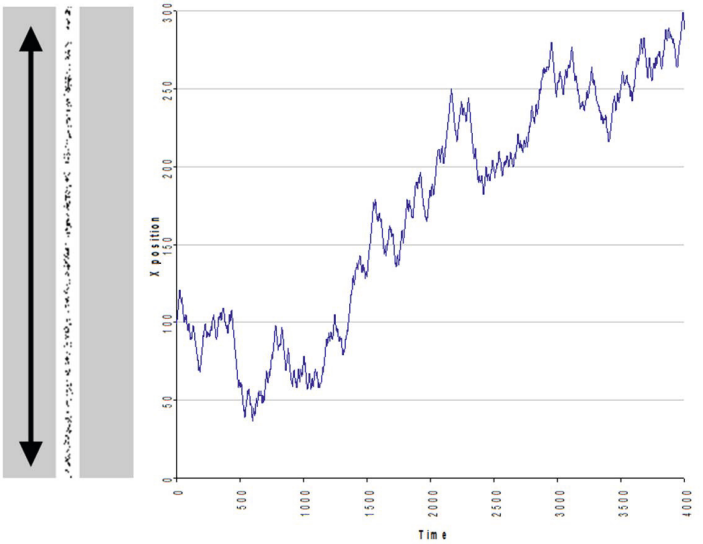

Fig. 3.6 Tracking of single particle shows characteristic shuttle streaming movement pattern. (Left) Particles confined in single path with periodic boundary, (Right) Plot of single particle X coordinate position over 4000 scheduler steps. P=300, SA 45°, RA 45°, SO 9.

3.6.3 Formation of Planar Sheet-Like Structures

It is also possible for the emergent agent networks to form uniform sheet-like structures. Fig. 3.7 shows the evolution of the stable SA 45°, RA 45° network without periodic boundary conditions. The agents again coalesce into network trails and the contraction behaviour condenses the network until all interior space is removed and a sheet-like mass remains. This sheet configuration also exhibits unusual properties: the sheet itself forms a minimal surface shape and ripple-like activity can be seen to propagate through the sheet (see supplementary recordings). The sheet also shows relatively stable dissipative 'islands' of greater trail flow. The islands reflect areas where a temporary vacancy of agents exists. The number and size of the islands is related to the sensor offset distance (SO) of the agents. When the SO parameter increases, the number of vacancy islands decreases and the spacing between them increases (Fig. 3.7). This suggests that the vacancy islands self-assemble based upon SO, agent positions and orientation and represent transient regions of free movement. The SA 22.5°, RA 45° networks also condense when boundary conditions are fixed, but no solid sheet-like mass is formed: the branching activity preventing network condensation into a complete sheet structure.

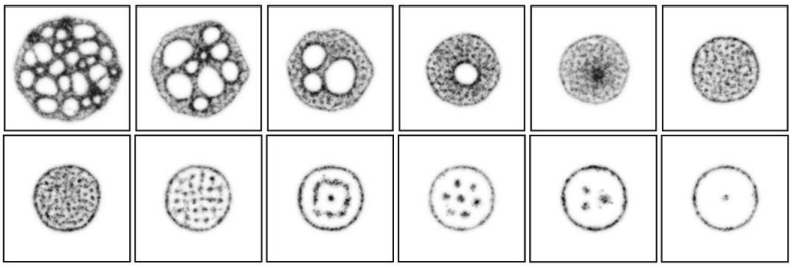

Fig. 3.7 Formation of sheet-like structures and the emergence of dissipative vacancy 'islands'. Top row (left to right) Network evolution over time: $\%p$ =20 agent trails, SA 45°, RA 45°. Bottom row (left to right) Dissipative vacancy island patterns at SO: 9, 13, 19, 23, 28, 38.

3.7 Factors Affecting Network Dynamics

There are a number of factors which affect the patterning and evolution of the emergent transport networks, which are discussed below.

3.7.1 Sensory Scale and Pattern Formation

The SO parameter (the distance in pixels between the agent position on the lattice and its three forward sensors) acts as a scaling factor. An example of how the SO parameter affects network formation can be seen in Fig. 3.8 for

SO distances of 3, 9, 15 and 25 pixels. The *SO* parameter affects the scaling of the patterns because the distance from the agent location to the position of the sensors reflects an indirect coupling between separate agents. When *SO* is small the agent receives sensory input from the chemical cues of only nearby agents and the coupling is weak. With large *SO* values the increased distance represents a strong coupling between distant agents. The stronger coupling results in coarser patterns with correspondingly large network structures and path thickness. In general terms very small sensor offset distances (*SO* 3 – 7) result in fine-grained network formation and evolution whilst larger offsets result in coarse-grained networks. As the network scale increases, so does the speed of network evolution. As the network paths are composed of agent particles, network paths formed by agents with larger *SO* have greater flux than those with smaller *SO*.

3.7.2 Population Density

The sensor scale may also affect the type of pattern formed, due to interplay with population density. At high population densities, there is less possibility of free agent movement (recall that agents only deposit chemoattractant when a move forwards is successful) and, as the sensor offset scale increases, there is a shift from network / lacunae pattern formation towards striped and spotted pattern formation (Fig. 3.9). The shift in pattern type at high population densities and large sensor scales is due to the fact that the agents free movement is restricted. The pattern of spots seen below (for example, at $\%p$ 90 and *SO* 27) is actually produced by the formation of vacancy domains — small regions of vacant space surrounded by areas solidly packed with immobile agent particles. At low $\%p$ the patterning is associated with areas of high agent occupancy (and movement) whereas at high $\%p$ the patterning is actually associated with areas of relatively low occupancy (but relatively free movement).

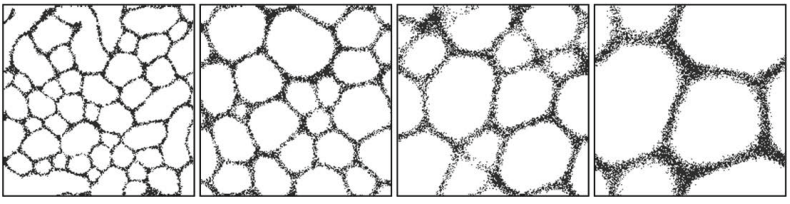

Fig. 3.8 Effect of Sensor Offset distance on pattern scale and granularity. Left to Right: Patterning produced with *SO* of 3, 9, 15, 25 pixels, Lattice 200×200. For all experiments: $\%p$=15, *SA* 45°, *RA* 45°, Evolution stopped at 500 steps.

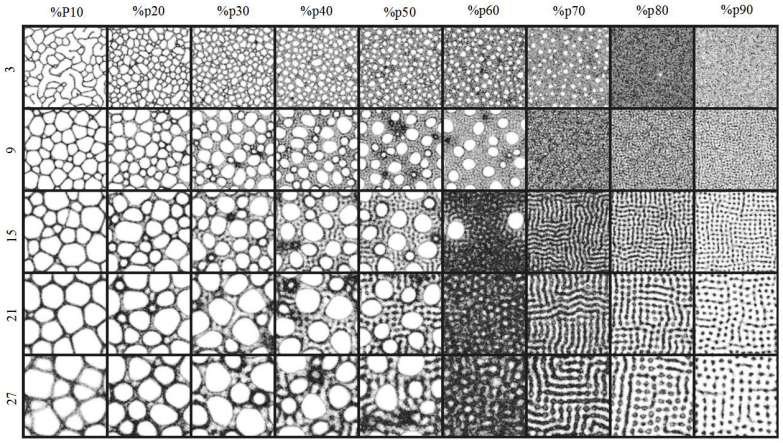

Fig. 3.9 Interaction between population size and sensory scale. Columns: $\%p$, Rows: SO distance, Lattice 300×300, SA 45°, RA 45°, Each experiment run for 500 steps.

3.7.3 Diffusion Properties

The pattern formation and evolution is also affected by the parameters which affect the diffusion of chemoattractant within the diffusion map, in terms of concentration, diffusion distance and gradient. Decreasing the damping factor D_d increases the concentration of chemoattractant in the diffusion map, as shown in Fig. 3.10. The increased concentration results in greater attraction of particles over a larger distance (bottom row). At low concentration the particle networks (top row) are more uniform in thickness, at high concentration the networks differ in thickness as clumps of particles aggregate together.

A decrease in D_d results in an increase in overall chemoattractant concentration and chemoattractant path width (Fig. 3.11a). The width of the diffusion kernel D_w also affected the peak height and width of the chemoattractant gradient. Larger kernels distributed the chemoattractant over a wider area, with a lower peak in concentration (Fig. 3.11b).

The diffusion damping parameter D_d affects the cohesion of the particle population. When a plasmodial sheet (a large mass of particles) is formed, the sheet is held together by the mutual attraction of particles to the chemoattractant flux produced by their own movement. The cohesion force minimises the approximate shape of the sheet to a circular form. This cohesion is also affected by the coupling provided by the SO parameter. The results in Fig. 3.12 demonstrate the effect of the damping parameter on the behaviour of a plasmodial sheet. Initially the sheet of particles has a D_d value of 0.05 (i) which results in strong cohesion. When D_d is increased to 0.1

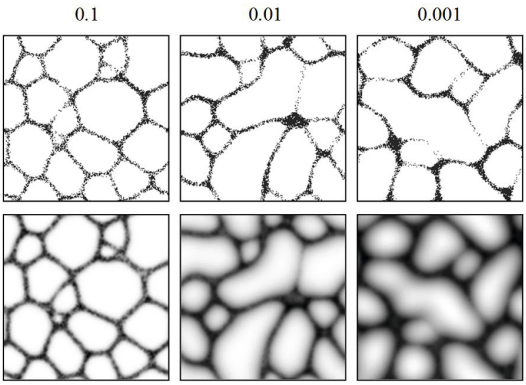

Fig. 3.10 Effect of chemoattractant concentration on network evolution. Top row: Transport networks composed of particle positions, Bottom row: Chemoattractant gradient concentration profile, $\%p$ 10, SA 45°, RA 45°, SO 9, D_d 0.1, 0.01 and 0.001. All experiments run for 500 steps.

(ii) the level of chemoattractant flux falls (see cross-section), as does the cohesion between the particles (visualised by the larger number of gaps between particles) but the cohesion is still strong enough to hold the sheet together. When D_d is increased to 0.5 (iii) the cross-section indicates that there are transient regions within the sheet where no flux is present. The breakdown in flux also occurs at the periphery of the sheet. Because there are regions where no cohesive force exists between the particles, and thus no difference in concentration between unoccupied regions of the environment and some parts of the plasmodial sheet, the approximately circular periphery of the sheet deforms and small pseudopodium-like filaments emerge (iv). These filaments extend and grow outwards from the main mass of particles. Decreasing the D_d parameter back to 0.1 restores the flux density above the zero level and restores cohesion to the mass of particles (v). The pseudopodium filaments begin to retract back into the mass of particles. Decreasing D_d to 0.05 increases the cohesion further (vi) until the plasmodial sheet regains its previous morphology.

The adaptation of the particle population to changing diffusion parameters mirrors the response of the *Physarum* plasmodium to changing environmental conditions. When nutrient conditions are poor the plasmodium extends pseudopodia into the nearby environment in an attempt to locate nutrients [124]. Conversely, when a plasmodium already occupies a rich source of nutrients, energy is conserved by remaining at that site until the nutrients are depleted [12]. The change in dynamical pattern formation by the model population suggests how the changes in the environment may play a direct role in the behaviour of an organism. This suggestion will be further explored in chapter 4.

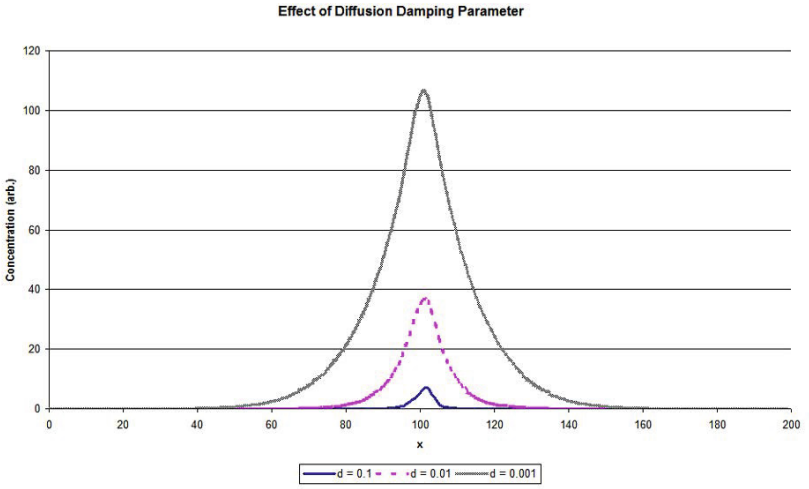

(a)

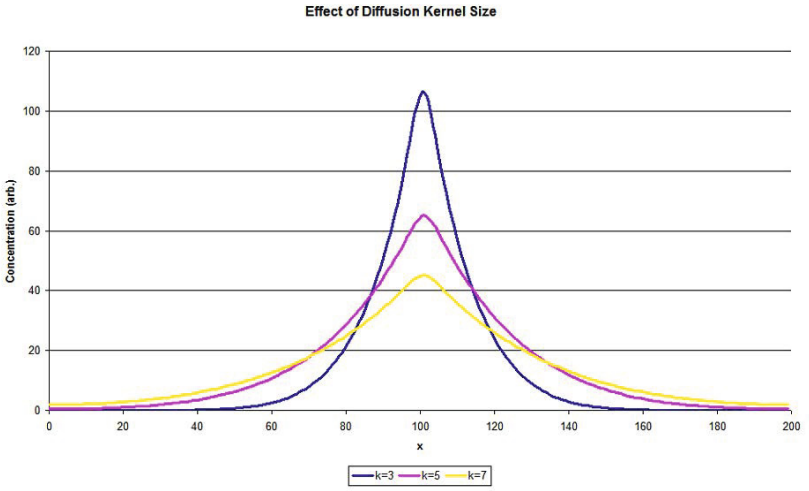

(b)

Fig. 3.11 Effect of diffusion damping and kernel size on chemoattractant distribution. (a) Decreased diffusion damping results in increased peak value and chemoattractant path width, (b) Decreased kernel size results in increased peak value and decreasing path width. p=500, SA 45°, RA 45°, SO 9, Dep_t 5, single vertical line of particles with periodic boundary.

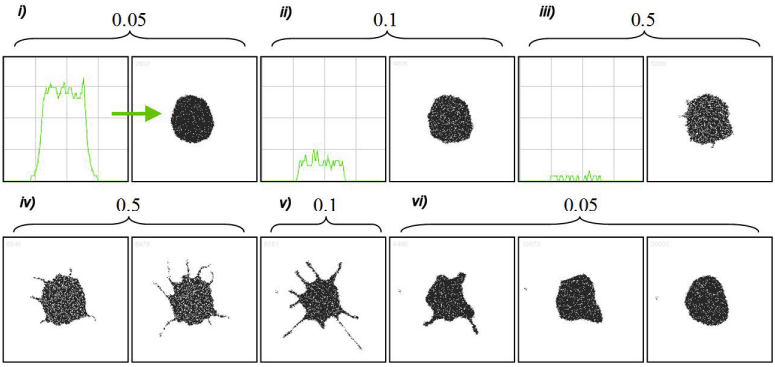

Fig. 3.12 Changes in cohesion result in pseudopodium extension and retraction. (Top row) Plot indicates chemoattractant concentration across arrowed line, (Bottom row) Extension and retraction of pseudopodia due to changes in cohesion (above).

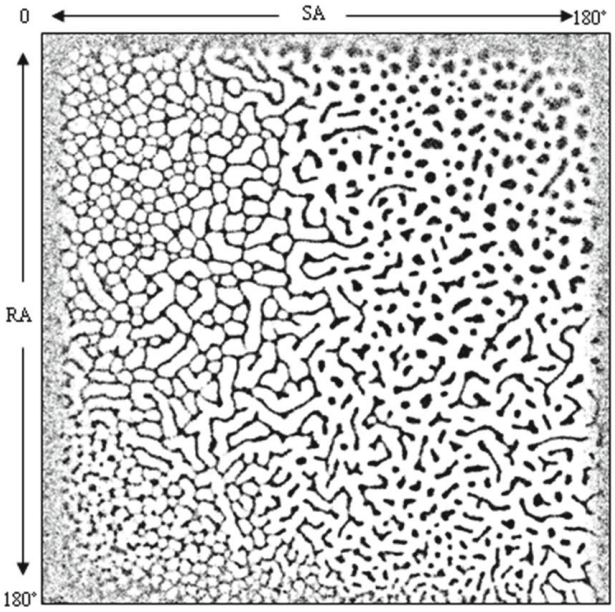

Fig. 3.13 Parametric mapping of SA and RA sensory parameters. $\%p$=20, SO 5, after 400 scheduler steps, SS 0.25 per step.

3.7.4 Sensor Angle and Rotation Angle

By adjusting the RA/SA parameters characteristic Turing-type patterns are generated. Fig. 3.13 illustrates the range of patterning when both RA and SA vary from zero to 180° on a fixed population size. A wide range of reaction-diffusion patterning including reticular, labyrinthine and spotted can be observed. The parameter ranges, particularly the sensor angle (SA), affects the cohesiveness of the population. At low SA (e.g. 22.5°) values there are dynamical branching reticular patterns. Increasing SA to 45° results in minimising reticular patterns. Further increases in SA result in labyrinthine and island patterns.

The emergent patterns invoked by the SA parameter are similar, at least superficially, to different pattern types observed in *Physarum* (reticulated networks, pseudopod-like extensions, sclerotium formation) under differing environmental conditions, such as those seen in [124]. This suggests that environmental variations such as substrate hardness, humidity and desiccation may affect the patterning mechanism within *Physarum* in a similar way Fig. 3.14.

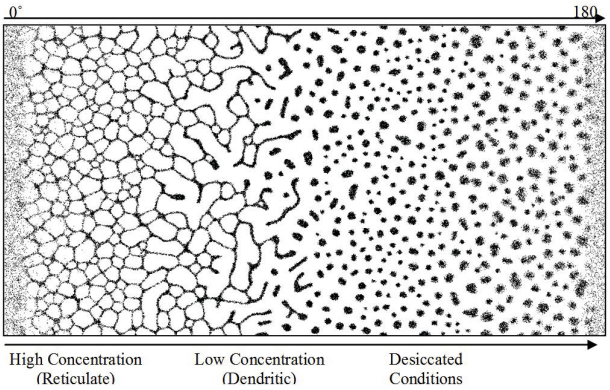

Fig. 3.14 SA parameter reproduces environmental conditions on plasmodium patterning. SA: 0-180°, RA 45°.

3.8 From Pattern Formation to Network Adaptation

The default behaviour of the emergent transport networks is a complex and dynamical pattern formation and evolution. Since it is possible to generate complex patterns without pre-existing cues, the presence of externally presented stimuli (pre-existing patterning cues) may be expected to guide, or modulate in some way, the underlying pattern formation process. Results of the particle population response to external (simulated nutrient) stimuli are

presented below. The nutrient stimuli are represented by sources of chemoattractant. The exact location of the source is represented by pixel locations in the agent environment lattice. The concentration of the stimulus is related to the pixel intensity of the stimulus, multiplied by the projection weight $Proj_d$. At each scheduler step locations that are marked by stimulus pixels were projected to the diffusive lattice. The projected stimuli are thus subject to the same diffusion process that applies to the agent produced chemoattractant. The weighting of the pre-pattern stimuli affects both the steepness and the area of the local concentration gradient (Fig. 3.15).

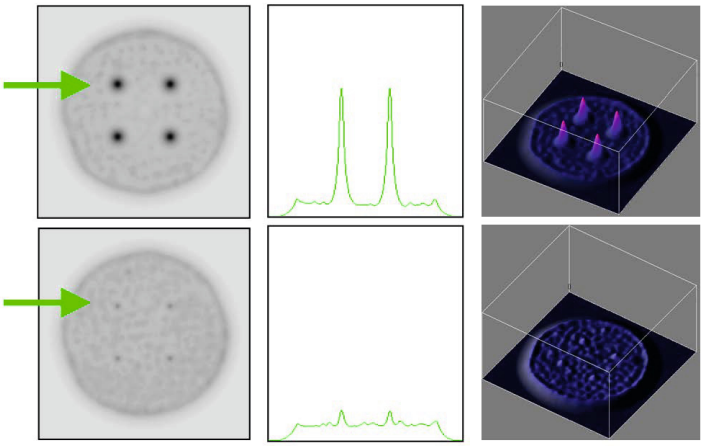

Fig. 3.15 Visualising external nutrient stimuli and the effect of stimuli weighting. (Left to right) Chemoattractant levels of a circular 'sheet' of agents with pre-pattern stimuli cues arranged as the four corners of a square, cross-section plot (indicated by arrow), 3D visualisation of chemoattractant concentration Pre-pattern projection weighting $Proj_d$: Top row = 0.06, bottom row = 0.01.

Because the projection stimuli are projected to the chemoattractant flux map, the stimuli act as sources of attractant to the agent population. An example of the effect of simple pre-pattern stimuli is shown in Fig. 3.16. When initialised with a small population size, the network initially emerges in the same way as previous examples. The network soon condenses around the strong chemotaxis stimuli presented by the two stimuli points in a similar effect to that seen by pins constraining soap film evolution [158], and the phenomenon of Zener pinning where dispersed particles affect the evolution of grain growth boundaries [164]. Using these points as an anchor, the network evolves until redundant paths are removed and the shortest path is left. When the number of stimulus sources is increased, the network evolution exhibits minimisation behaviour characteristic of minimum Steiner tree formation (for a given set of points, the Steiner tree represents the shortest amount of connecting material when all points are connected). The tree is

formed when redundant network paths are shortened and closed by the emergent minimisation effects (Fig. 3.17). The supplementary recordings illustrate that the network converges on the final tree shape, despite often following very different dynamic graph trajectories.

3.9 Factors Affecting Network Adaptation

To examine the factors affecting evolution we assessed the simplest case of a three node network where a central node is surrounded by two outer nodes at equal distance and equal angles. A small population (100) was initialised on a horizontal line spanning the three nodes (see scheme in Fig 3.18a).

Initially the angle between the two outer nodes was 180° and this angle was systematically decreased at regular intervals (one degree every 200 scheduler steps), pivoting the outer nodes around the central nodes. When a critical angle was reached the two outer network paths touched near the vicinity of the central node and merged. The mutual attraction of the flows pulled the network away from the central node and the direct connection to the central node was broken by the characteristic 'zipping' motif. The zipping behaviour continued until the three competing network flows stabilised at a Steiner point. The critical angle was measured at different nutrient $Proj_d$ of 0.005, 0.05, 0.5 and 5, and at different SO scales of 5, 9 and 13 pixels. A summary of the results is shown in Fig 3.18b.

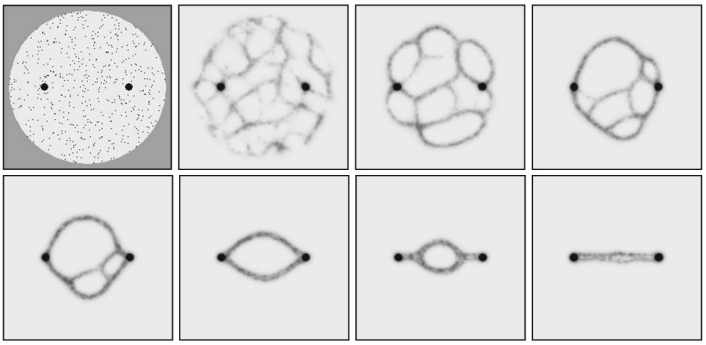

Fig. 3.16 Pattern formation and evolution under the influence of nutrient stimuli. 200×200 lattice, $\%p$ 2, SA 45°, RA 45°, SO 9, (Top Left) Environment shows: pre-pattern cues (dark spots), initial agent positions (small grey flecks) and boundary of the environment (uniform grey), Remaining images (left to right): Evolution of network formation as the network becomes 'snagged'. Minimisation of the network continues until the shortest path between the stimuli remains.

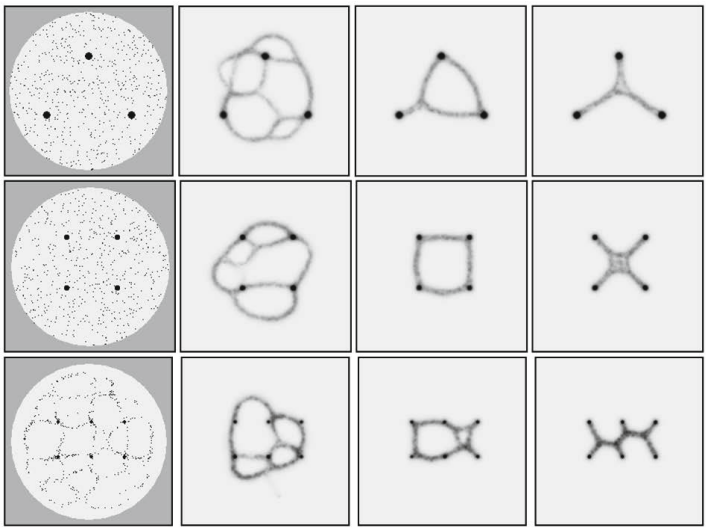

Fig. 3.17 Approximation of Steiner minimum trees in simple nutrient stimuli arrangements. Lattice 200×200, SA 45°, RA 45°, SO 9, $\%p$=2 (except bottom row, $\%p$=1.25).

The results summarised in the chart indicate that both $Proj_d$ and SO affect the size of the critical angle. Increasing SO distance resulted in the critical angle occurring at larger angles than with smaller SO. This is because a larger sensor offset distance results in thicker network paths and these paths come into proximity with each other at relatively larger network angles. The effect of nutrient concentration, via $Proj_d$ is more pronounced. Smaller weights do not exert as great an influence on the network paths as do larger weights (indeed at SO 5 and $Proj_d$ 0.005 the attraction of the nodes was not strong enough to constrain the paths reliably, resulting in serpentine foraging network paths, and no information on the critical angle could be obtained). At high projection weights the influence of the nodes resulted in a much smaller critical angle and also a wider region of influence on nearby network paths. Very high concentration could even 'unzip' nearby Steiner points, returning the connections to the node itself. The wide region of influence at high concentration is analogous to the influence of different peg diameters in soap film minimisation schemes [165]. High concentration stimuli take the form of a circular area of relatively large diameter which separates the two outer paths connecting to the circle, thus the critical angle can be reduced to a smaller value before the paths contact and merge. Low concentration stimuli result in a smaller stimulus area which is not able to separate the two outer paths to the node, resulting in a larger critical angle before the paths merge.

Although the findings illustrate the critical angle for evolution around a single node of the network it should be emphasised that changes to a single

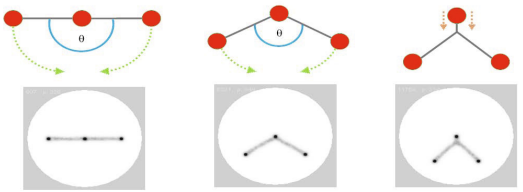

(a)

(b)

Fig. 3.18 Node detachment angle influenced by sensor scale and nutrient node concentration. (a) Schematic illustration of experimental evolution (top), and experimental snapshots (bottom). Rightmost image shows example just after critical angle has been exceeded and unzipping starts. (b) Plot of critical sensor angle thresholds at different node concentration and sensor offset distances.

node position can have a significant impact on the evolution of the entire network. This is because when the network configuration changes (by zipping away from a node when a critical angle between two outer nodes is reached) this reconfiguration subsequently affects the node angles at other locations in the network. The effects are compounded when one takes into consideration that the network evolution is continuing at all parts of the network simultaneously. The final configuration (if indeed the word final can be used, since the configuration consists of dynamical network flows) only occurs when the flows in the entire network are balanced.

3.10 Observation of von Neumann's Law and Plateau Angles

The evolution of contractile networks shows characteristic evolution dynamics which approximate those observed in soap films, froths and grain growth [157], and lipid nanotube networks [111]. The global dynamics are composed of individual transformations between cells (of lacunae) in the network. A topological reconfiguration known as a $T2$ relaxation process is observed when a lacuna surrounded by three paths shrinks (Fig. 3.19, top row). When the lacuna has completely closed the resulting Steiner point stabilises between the three nodes at a typical angle of 120°, demonstrating Plateau angles (a more complete analysis of angle distributions is given in chapter 4). $T1$ topological processes are observed when the four or more paths merge (Fig. 3.19, second row). The four way junction is not stable and the paths separate, forming a new edge whose extension continues until the network approximates the Steiner minimum tree.

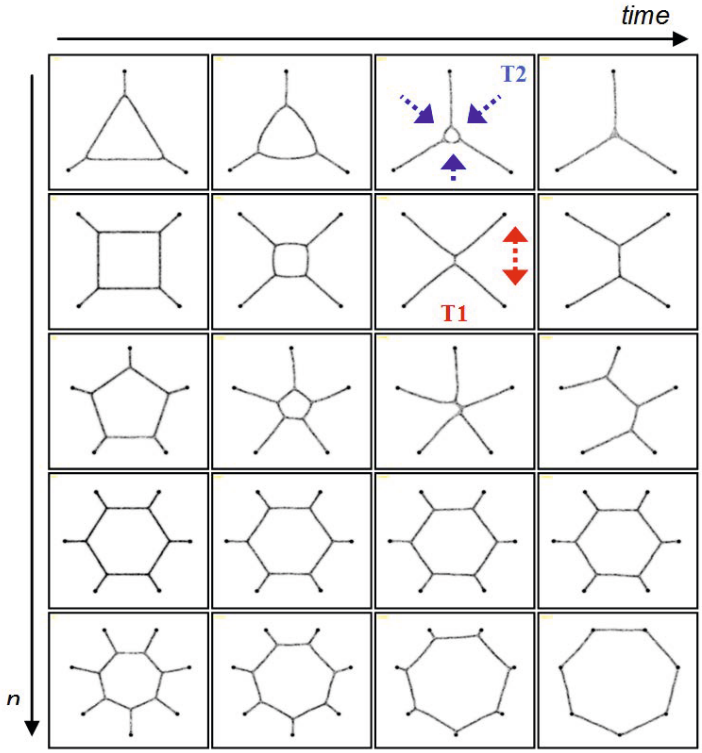

Fig. 3.19 $T2$ and $T1$ relaxation processes, Plateau phenomena, and von Neumann's law. n represents number of nodes and edges (For explanation of T2 and T1 evolution see text).

When the number of nodes increases, network evolution is a complex combination of $T2$ and $T1$ processes (for example in Fig. 3.19, third row there is a $T2$ process relaxation which results in the expansion of two separate $T1$ processes). For regular configurations the network evolution observes von Neumann's law where cells with sides $n < 6$ shrink, cells with $n > 6$ six sides grow in size, and cells where $n = 6$ maintain the same shape.

3.11 Summary — A Virtual Plasmodium

We approximate *Physarum* using a fine-grained bottom-up approach as the coupled interaction of components within the actomyosin matrix. We do not consider the complex chemical and energetic transformations responsible for the individual contractile forces within the plasmodium. However we do consider the local coupling mechanisms by which the individual contractile forces interact. We thus assume that the complex and dynamical patterning of the *Physarum* plasmodium is an emergent property caused by the gel/sol interactions.

We use a multi-agent method in which we couple a population of simple mobile agents to a diffusive chemoattractant lattice. Individual hypothetical units of gel and sol interaction are represented by a single agent particle. Collectively, the combined position and pattern of the population represents the entire plasmodium. The position of the particle represents the presence of plasmodium at a location and the movement of a particle represents protoplasmic flux at a location. The concentration of chemoattractant at individual lattice sites represent the level of protoplasmic flux at each site in the lattice.

The particle population collectively exhibits complex, emergent and dynamical pattern formation by self-organised interactions. The pattern formation behaviour corresponds to the spontaneous pattern formation seen in the *Physarum* plasmodium and, from a broader perspective, approximates a wide range of Turing-like patterning. We found that the emergent transport networks formed by the model exhibited quasi-physical second order properties during their complex evolution, showing complex network adaptation and minimisation and specific motifs within the complex evolution of the networks. These motifs included network branching, network path anastomoses, zipping/unzipping of paths and bi-directional movement approximating shuttle streaming. A comprehensive parametric evaluation characterised the behaviour of the model under a variety of sensory parameter combinations, demonstrating different pattern types and changes in pattern scale. The effect of environmental conditions was explored, including crowding effects in large populations and the effect of diffusion parameters on population cohesion. We examined the effect of nutrient placement, critical angles between nutrients, and nutrient concentration on network adaptation. The quasi-physical behaviours were found to observe Plateau's phenomena of 120° angles at Steiner junctions and the emergence of network relaxation processes adhered to von Neumann's law.

The base collective behaviour of the model is that of a virtual material which, by virtue of its complex *Physarum*-like patterning and network adaptation, we may term a 'Virtual Plasmodium'. In the next chapter we show how the base model behaviour may be used to reproduce the complex biological behaviour seen in *Physarum* under a range of environmental conditions.